ISSN 1070-3284, Russian Journal of Coordination Chemistry, 2015, Vol. 41, No. 1, pp. 37–42. © Pleiades Publishing, Ltd., 2015.
Original Russian Text © E.A. Katlenok, A.A. Zolotarev, K.P. Balashev, 2015, published in Koordinatsionnaya Khimiya, 2015, Vol. 41, No. 1, pp. 40–45.

Iridium(III) and Platinum(II) Complexes with Metallated and Chelating Benzothiazole Derivatives: Structural, Optical, and Electrochemical Properties

E. A. Katlenok[a], A. A. Zolotarev[b], and K. P. Balashev[a, *]

[a] *Russian State Pedagogical University, St. Petersburg, Russia*

[b] *St. Petersburg State University, St. Petersburg, Russia*

**e-mail: balashevk@mail.ru*

Received May 20, 2014

Abstract—The structures of the Ir(III) and Pt(II) complexes with metallated 2-phenylbenzothiazole (Bt) and chelating 2-(2-hydroxo)phenylbenzothiazole (Hbt) in the crystalline state and in a $CDCl_3$ solution are studied by X-ray diffraction analysis and ^1H NMR spectroscopy. The structures of the complexes are shown to be *cis*-C,C-[$Ir(Bt)_2(HBt)$] (**I**) and *trans*-N,N-[Pt(Bt)(HBt)] (**II**) (CIF files CCDC 996857 (**I**) and 995845 (**II**)). Based on the results of absorption and emission electron spectroscopy, the highest occupied and lowest unoccupied molecular orbitals (HOMO and LUMO) determining the character of long-wavelength optical bands and electrochemical processes are assigned to the orbitals predominantly localized on the {Ir(Bt)} fragment for complex **I**, whereas for complex **II** the LUMO is localized on {Pt(Bt)} and the HOMO is localized on the {Pt(HBt)} fragment.

DOI: 10.1134/S1070328415010042

INTRODUCTION

Phosphorescence at room temperature and reversibility of the electrochemical out-of-sphere electron transfer processes of the cyclometallated Pt(II) and Ir(III) complexes are of increased interest [1, 2] because of wide prospects of using in organic light diodes [3], photocatalysts [4], luminescent labels of biosystems [5], and chemosensors [6]. The benzothiazole derivatives characterized by the N and S donor atoms form coordinatively unsaturated complexes–ligands capable of donor–acceptor interacting with an additional metal cation. Therefore, they are promising for the development of metallocomplex sensors to heavy metals based on these compounds [7].

In this work, we studied the molecular structures and the optical and electrochemical properties of complexes [$Ir(Bt)_2(Hbt)$] (**I**) and [Pt(Bt)(HBt)] (**II**) with metallated 2-phenylbenzothiazole ({M(Bt)}) and chelating 2-(2-hydroxo)phenylbenzothiazolate ion (HBt)

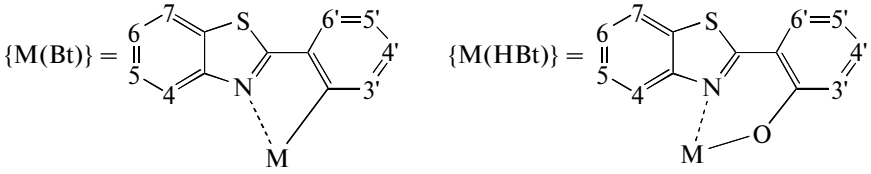

EXPERIMENTAL

Complexes **I** and **II** were synthesized in ~50% yield and their single crystals were obtained similarly to described procedures [7, 8] using available reagents (reagent grade).

The ^1H NMR spectra of complexes **I** and **II** in $CDCl_3$ solutions were recorded on a JNM-ECX400A spectrometer (Center for Collective Use, Department of Chemistry, Russian State Pedagogical University, St. Petersburg).

^1H NMR, δ, ppm: for (2-(2-hydroxo)phenylbenzothiazolato)bis(2-phenyl-3-ido)benzothiazole)iridium (**I**), {Ir(HBt)}: 7.23 d, 7.08 dd, 6.98–6.91 m (4 H), 6.59 dd, 6.48 d; $\{Ir(Bt)_2\}$: 8.82 dd, 7.79 dd, 7.90 d, 7.70 d, 7.68 d, 7.59 d, 7.29 td, 7.13 td, 6.98–6.85 m (4 H),

Table 1. Crystallographic and refinement parameters for the structures of complexes **I** and **II**

Parameter	**I**, $[Ir(Bt)_2(HBt)]$	**II**, [Pt(Bt)(HBt)]
Empirical formula	$C_{39}H_{24}N_3OS_3Ir$	$C_{26}H_{16}N_2OS_2Pt$
FW	838.99	631.62
Crystal system	Monoclinic	Monoclinic
Space group	$P2_1/c$	$P2_1/c$
Unit cell parameters		
a, Å	11.5207(7)	10.9485(4)
b, Å	15.0507(7)	13.7413(5)
c, Å	18.4118(10)	13.9391(5)
β, deg	102.859(6)	90.961(3)
V, Å^3; Z	3095.5(3); 1	2096.8(1); 1
ρ_{calcd}, g/cm^3	1.800	2.001
μ, mm^{-1}	4.555	6.914
F(000)	1648.0	1216.0
2θ Range, deg	5.16–55	5.56–54
Index range	$-11 \le h \le 14$, $-19 \le k \le 18$, $-23 \le l \le 23$	$-13 \le h \le 11$, $-17 \le k \le 16$, $-17 \le l \le 17$
Total number of reflections	28653	10543
Number of independent reflections (R_{int})	7006 (0.0527)	4432 (0.0421)
Goodness-of-fit	1.033	1.046
R factors ($\|F_o\| \ge 4\sigma(F)$)	$R_1 = 0.0325$, $wR_2 = 0.0584$	$R_1 = 0.0355$, $wR_2 = 0.0742$
R factors (all data)	$R_1 = 0.0480$, $wR_2 = 0.0627$	$R_1 = 0.0462$, $wR_2 = 0.0805$
ρ_{min}, ρ_{max}, e Å^{-3}	–0.69, 1.39	–0.69, 1.39

$R_1 = \Sigma\|F_o| - |F_c\|/S|F_o|$; $wR_2 = \{\Sigma[w(F_o^2 - F_c^2)^2]/\Sigma[w(F_o^2)^2]\}^{1/2}$; $w = 1/[\sigma^2(F_o^2) + (aP)^2 + bP]$; $P = (F_o^2 + 2F_c^2)/3$; $s = \{\Sigma[w(F_o^2 - F_c^2)]/(n - p)\}^{1/2}$, n is number of reflections, and p is number of refines parameters.

6.75 td, 6.71 td, 6.23 d, 6.09 dd; for (2-(2-hydroxo)phenylbenzothiazolato)((2-phenyl-3-ido)benzothiazole)platinum (**II**), {Pt(HBt)}: 7.83 d, 7.82 m, 7.44 d, 7.41–7.38 m (2 H), 6.99 dd, 6.70 d, 6.59 t; {Pt(Bt)}: 9.84 d, 8.34 m, 7.66 dd, 7.51 dd, 7.47 dd, 7.28 td, 7.10 d, 6.75 td.

Absorption and emission spectra were recorded on an SF-2000 spectrometer and a Flyuorate-02-Panorama spectrofluorimeter. Voltammograms were obtained on an IPC-PRO system in a cell with divided spaces of the working (glassy carbon), auxiliary (Pt), and reference (Ag) electrodes in the presence of 0.1 M $[N(C_4H_9]PF_6$ in a $C_6H_5CH_3$–CH_3CN (1 : 1) mixture. The peak potentials were presented with respect to the ferrocenium–ferrocene redox system at a rate of 100 mV/s.

X-ray diffraction analysis was carried out at 100 K on an AgilentTechnologiesExcaliburEos single crystal diffractometer (Resource Center "X-Ray Diffraction Investigation Methods" of the St. Petersburg State University) equipped with a reflected X-ray beam planar detector of the CCD type (MoK_α radiation, λ = 0.71073 Å). The crystallographic data and refinement parameters for structures **I** and **II** are given in Table 1. The unit cell parameters were refined by the least-square method. The structures were solved by direct methods and refined using the SHELXL program [9] in the OLEX2 program package [10] by the full-matrix least-square method in the anisotropic approximation. An absorption correction was applied in the CrysAlisPro program package [11]. Hydrogen atoms were included in refinement with fixed temperature parameters. The CIF files containing information on the structures of the complexes were deposited with the Cambridge Crystallographic Data Centre (CCDC nos. 996857 (**I**) and 995845 (**II**); www.ccdc.cam.ac.uk/data_request/cif).

RESULTS AND DISCUSSION

The crystalline lattices of complexes **I** and **II** (Fig. 1) contain *cis*-C,C-[Ir(Bt)$_2$(HBt)] and *trans*-N,N-[Pt(Bt)(HBt)] isomers typical of the cyclometallated Ir(III) and Pt(II) compounds with chelating ligands [7, 12]. The distance equal to 2.31 Å between O(HBt) and H(7)(Bt) in the isomer of compound **II** indicates the intramolecular hydrogen bond. The bonds at the donor atoms of the C- and N-metallated 2-phenylbenzothiazole ligands in complex **I** are elongated by 0.01–0.02 Å compared to those in complex **II** (Table 2). Due to a higher *trans*-effect of the C atom compared to that of the N atom of metallated 2-phenylbenzothiazole, the bond length of the chelating HBt$^-$ ligand, which is in the *trans* positions to the C and N atoms for complexes **I** and **II**, differs by 0.21 Å. A similar *trans* position to the C atom of the O donor atom in complexes **I** (Ir(III)) and **II** (Pt(II)) determines a significantly lower difference (by 0.05 Å) in the bond length of the O atom with the metal.

The sum of bond angles of the donor atoms of the ligands at the Pt atom (359.9°) corresponds to the square coordination of the platinum atom in complex **II**. Unlike the metallated ligand, whose benzothiazole and phenyl components deviate from the coordination plane by no more than 2.6°, the benzothiazole and phenyl components of chelating HBt$^-$ deviate from the coordination plane by 24° and 31°, respectively.

The sum of bond angles at the C(Bt), N(HBt), O(HBt), C(Bt), and N(Bt) atoms in the equatorial plane is 360.1°. The deviation of the axial N(Bt) ligands from the perpendicular position to the equatorial plane by 10° results in the distortion of the octahedral coordination mode of the Ir atom in complex **I**. The benzothiazole and phenyl components of the metallated 2-phenylbenzothiazole ligands deviate from the planes of Ir, C(Bt), and N(Bt) by 12°–20° and 6°–20°, respectively. The benzothiazole and phenyl components of Hbt$^-$ deviate from the Ir, N(HBt), O(HBt) plane by 20° and 44°, respectively.

The results of ^{1}H NMR spectroscopy for complexes **I** and **II** in a $CDCl_3$ solution show that they retain the molecular structures that were determined in the crystalline state. The *trans*-N,N-[Pt(Bt)(HBt)] and *cis*-C,C-[Ir(Bt)$_2$(HBt)] isomers of complexes **II** and **I** are characterized by 16 and 24 signals, respectively, from protons of the ligands. According to the structure of *trans*-N,N-[Pt(Bt)(HBt)], the protons of the benzothiazole component of the metallated ligand undergo a downfield shift compared to the free ligand (Table 3). The upfield shift of the signals from the protons of the chelating ligand by 0.2–0.1 ppm is due, most likely, to the anisotropic influence of the circular current of the phenyl ring *cis*-arranged at an angle of 13.8° at a distance of 3 Å.

The magnetic nonequivalence of two metallated ligands in the composition of compound **I** and a signif-

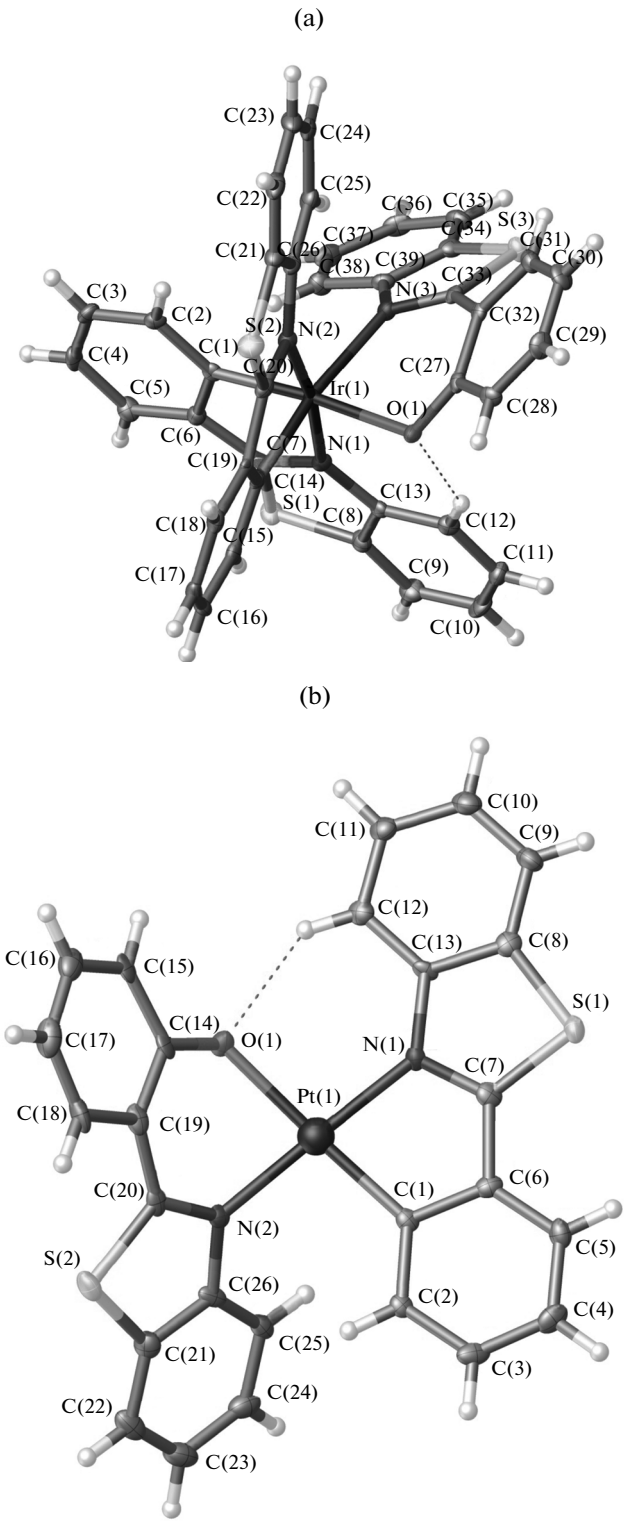

Fig. 1. Molecular structures of complexes (a) [Ir(Bt)$_2$(HBt)] (**I**) and (b) [Pt(Bt)(HBt)] (**II**) in the crystalline lattice.

Table 2. Bond lengths and bond angles for complexes **I** and **II**

Bond	*d*, Å	
	I	**II**
M–C(1,14)(Bt)	2.002(5), 2.010(3)	1.999(6)
M–N(1,2)(Bt)	2.041(3), 2.054(3)	2.021(4)
M–N(3)(HBt)	2.221(3)	2.008(4)
M–O(1)(HBt)	2.151(2)	2.100(3)
Angle	ω, deg	
	I	**II**
C(1,14)(Bt)MN(1,2)(Bt)	80.1(1), 80.3(1)	80.4(2)
C(1,14)(Bt)MN(2,1)(Bt)	96.1(1), 92.3(1)	
N(1,2)(Bt)MO(1)(HBt)	98.7(1), 84.4(1)	97.8(2)
O(1)(HBt)MN(3)(HBt)	84.9(1)	83.6(2)
N(3)(HBt)MC(1,14)(Bt)	100.4(1), 171.2(7)	98.1(2)
C(1)(Bt)MC(14)(Bt)	88.4(1)	
N(1,2)(Bt)MN(3)(HBt)	88.0(1), 99.9(1)	178.5(2)
C(1,14)(Bt)MO(1)(HBt)	86.4(1), 174.5(1)	173.2(2)
N(1)(Bt)MN(2)(Bt)	171.8(1)	

icant upfield chemical shift of the H(3)' protons due to the mutual anisotropic effect of circular currents of the phenyl rings of the metallated ligands (Table 3) confirm that the complex exists in the form of the *cis*-C,C isomer. In accord with the *trans* position of the C atoms of the metallated ligands and donor O and N atoms of chelating HBt^-, the resonances of protons of their benzothiazole and phenyl components undergo upfield shifts.

The absorption spectra of complexes **I** and **II** contain bands of different nature (Table 4). In the short-wavelength region at 230–330 nm the complexes are characterized (Fig. 2) by highly intense ($\varepsilon = 4–2 \times 10^4$ L mol^{-1} cm^{-1}) bands, whose position almost coincides with the absorption of the free ligands [7, 13]. Therefore, they can be assigned to intraligand (IL) π–π* optical transitions. Less intense ($\varepsilon \approx 1 \times 10^4$ L mol^{-1} cm^{-1}) and typical of the cyclometallated complexes with metallocomplex fragments {Pt(Bt)} and {Ir(Bt)$_2$} [14, 15] bands at 350–425 and 370–540 nm were ascribed to the metal–metallated ligand charge transfer (MLCT) d_π–π*(Bt). The longest-wavelength shoulder at 458 sh ($\varepsilon \approx 5.8 \times 10^3$ L mol^{-1} cm^{-1}) in the spectrum of complex **II** was attributed to the ligand-to-ligand charge transfer (π*(Bt) → π*(HBt)) involving the π* orbitals of the metallated and chelating ligands.

The photoexciatation of solutions of the complexes in dichloromethane ($\lambda_{exc} = 400$ nm) results (Fig. 2) in their weakly structured phosphorescence in the visible region. The phosphorescence spectrum of complex **I** with a maximum at 677 nm is bathochromically shifted compared to that of [Ir(Bt)$_2$(Acac)] (**III**), where $Acac^-$ is the acetylacetonate ion [15], by less than 300 cm^{-1}, indicating a similar MLCT/IL mixed nature of the spin-forbidden optical transition predominantly localized on the metallocomplex fragment {Ir(Bt)$_2$}. Unlike complex **I**, the maximum of the phosphorescence spectrum of complex **II** at 578 nm is bathochromically shifted compared to the spectrum of complex [Pt(Bt)(Acac)] (**IV**) [16] by more than 1200 cm^{-1}. This indicates a change in the nature of the mixed IL/MLCT spin-forbidden optical transition localized on the {Pt(Bt)} fragment and assumes that the orbitals of the {Pt(HBt)} component of complex **IV** participate in the optical transition.

Under the assumption that the Koopmans theorem [17] is valid for compounds **I** and **II**, one can expect a similarity of the HOMO and LUMO responsible for the nature of the long-wavelength absorption and electrochemical oxidation and reduction processes of the complexes. The voltammograms of complex **I** are characterized by typical waves of one-electron and irreversible oxidation and reduction processes with

Table 3. Coordination-induced chemical shifts ($\Delta = \delta_{complex} - \delta_{free\ ligand}$, ppm) of the H atoms of complexes **I** and **II** in $CDCl_3$

Complex	H(4)	H(5)	H(6)	H(7)	H(3)'	H(4)'	H(5)'	H(6)'
{M(Bt)}								
[Ir(Bt)$_2$(HBt)] (**I**)	0.7/–0.3	–0.4/–0.6	–0.2/–0.6	–0.2/–0.5	–1.3/–0.8	–1.3/–0.6	–0.8/–0.7	–0.4/–0.4
[Pt(Bt)(HBt)] (**II**)	1.7	0.2	0.0	0.2	–0.4	–0.1	–0.8	–0.6
{M(HBt)}								
[Ir(Bt)$_2$(HBt)] (**I**)	–1.5	–0.3	–0.4	–1.0	–0.2	–0.4	–0.6	–0.5
[Pt(Bt)(HBt)] (**II**)	–0.2	0.0	0.0	–0.1	–0.4	–0.4	–0.5	–0.3

Table 4. Optical and electrochemical characteristics of complexes **I** and **II***

Complex	Absorption λ_{max}, nm ($\varepsilon \times 10^3$ L mol^{-1} cm^{-1})	Emission λ_{max}, nm	Oxidation E_p, V	Reduction E_p, V
I	257 (42.7), 278 (40.6), 318 (33.8), 371 (12.7), 424 (10.1), 452 sh (9.5), 502 sh (5.0), 540 sh (2.3)	566, 606 sh, 677 sh	0.45	−2.32
II	233 (39.7), 270 (33.7), 316 (23.4), 330 sh (20), 350 sh (10), 387 sh (7.4), 414 sh (9.7), 426 (10.1), 458 sh (5.8)	540 sh, 578, 604 sh, 638 sh, 677 sh	0.60	−2.17

* $CDCl_3$ are optical, and $C_6H_5CH_3$–CH_3CN (1 : 1) are electrochemical.

potentials (E_p) close to those of complex **III** [18]. This makes it possible to assign the oxidation and reduction waves of complex **I** to similar metal- and ligand-centered electrochemical processes involving the *d* orbital of Ir

$$[Ir^{III}(Bt)_2(Hbt)] - e^- \rightarrow [Ir^{IV}(Bt)_2(Hbt)]^+$$

and the π* orbital of the metallated ligand

$$[Ir(Bt)_2(Hbt)] + e^- \rightarrow [Ir(Bt)(Bt^-)(Hbt)]^-.$$

The irreversible one-electron reduction of compound **II** is observed at −2.17 V. This is consistent with the ligand-centered character of the electron transfer to the π* orbital of the metallated ligand

$$[Pt(Bt)(HBt)] + e^- \rightarrow [Pt(Bt^-)(HBt)]^-.$$

The cathodic shift of the current potential of the oxidation peak of compound **II** compared to the metal-centered oxidation of $[Pt(Bt)(En)]^+$ (En is ethylenediamine) by ~0.5 V indicates a change in the nature of the HOMO involved in the electrochemical oxidation. The ligand-centered character of the oxidation of complex **II** involving the *p* orbital of the donor oxygen atom

$$[Pt(Bt)(HBt)] - e^- \rightarrow [Pt(Bt)(HBt^+)]$$

can be assumed due to the effective interaction of the Pt atom with this deprotonated O atom of the chelating ligand.

The results obtained show the *cis*-C,C-$[Ir(Bt)_2(Hbt)]$ and *trans*-N,N-[Pt(Bt)(HBt)] structures of complexes **I** and **II**, respectively. Their optical and electrochemical properties are determined by the similar nature of the LUMO predominantly localized on the π* orbitals of the metallated ligand but different natures of the metal-centered HOMO for complex **I** (*cis*-C,C-$[Ir(Bt)_2(HBt)]$) and ligand(HBt)-centered HOMO for complex **II** (*trans*-N,N-[Pt(Bt)(HBt)]).

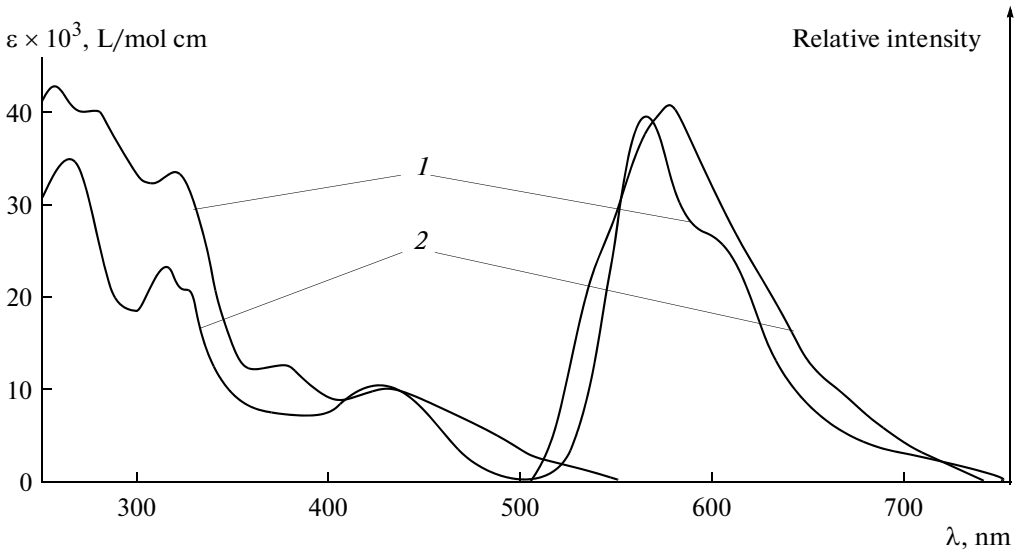

Fig. 2. Absorption and emission spectra of complexes (*1*) $[Ir(Bt)_2(HBt)]$ and (*2*) [Pt(Bt)(HBt)] in a CH_2Cl_2 solution.

ACKNOWLEDGMENTS

This work was supported by the Ministry of Education and Science of the Russian Federation (state program no. 4.131.2014K).

REFERENCES

1. Albrecht, M., *Chem. Rev.*, 2010, vol. 110, p. 576.
2. You, Y. and Nam, W., *Chem. Soc. Rev.*, 2012, vol. 41, no. 21, p. 7061.
3. Chi, Y. and Chou, P.T., *Chem. Soc. Rev.*, 2010, vol. 39, no. 3, p. 638.
4. Kubas, G.J., *J. Organomet. Chem.*, 2009, vol. 694, no. 17, p. 2648.
5. Leung, C.-H., Zhong, H.-J., Chan, D.S.H., and Ma, D.-L., *Coord. Chem. Rev.*, 2013, vol. 257, nos. 11–12, p. 1764.
6. Zhao, Q., Li, F., and Huang, C., *Chem. Soc. Rev.*, 2010, vol. 39, no. 8, p. 3007.
7. Liu, Y., Zhao, Q., Wu, H., et al., *Inorg. Chem.*, 2011, vol. 50, no. 13, p. 5969.
8. Katlenok, E.A. and Balashev, K.P., *Russ. J. Gen. Chem.*, 2012, vol. 82, no. 9, p. 1583.
9. Sheldrick, G.M., *Acta Crystallogr., Sect. A: Found. Crystallogr.*, 2008, vol. 64, no. 1, p. 112.
10. Dolomanov, O.V., Bourhis, L.J., Gildea, R.J., et al., *J. Appl. Crystallogr.*, 2009, vol. 42, no. 2, p. 339.
11. CrysAlisPro. Agilent Technologies. Version 1.171.36.20 (release 27-06-2012).
12. Kvam, P.-I., Engebretsen, T., Maartmann-Moe, K., et al., *Acta Chem. Scand.*, 1995, vol. 50, p. 107.
13. Katlenok, E.A., Ivanova, E.V., Puzyk, M.V., et al., *Opt. Spektrosk.*, 2012, vol. 113, no. 3, p. 311.
14. Katlenok, E.A. and Balashev, K.P., *Opt. Spektrosk.*, 2013, vol. 114, no. 5, p. 824.
15. Lamansky, S., Vrettos, J.S., Crantree, R.H., et al., *Inorg. Chem.*, 2001, vol. 40, no. 7, p. 1704.
16. Laskar, I.R., Hsu, S.-F., and Chen, T.-M., *Polyhedron*, 2005, vol. 24, no. 8, p. 881.
17. Koopmans, T., *Physics*, 1933, vol. 1, no. 1, p. 104.
18. Wu, Y., Jing, H., Dong, Z., et al., *Inorg. Chem.*, 2011, vol. 50, no. 16, p. 7412.

Translated by E. Yablonskaya